Oxidation of 2,4-dichlorophenol in saline water by unactivated peroxymonosulfate: Mechanism, kinetics and implication for in situ chemical oxidation

Zeng Huabin, Zhao Xu, Zhao Feiping, Park Yuri, Repo Eveliina, Thangaraj Senthil K., Jänis Janne, Sillanpää Mika

DOI: 10.1016/j.scitotenv.2020.138826

Oxidation of 2,4-Dichlorophenol in Saline Water by Unactivated Peroxymonosulfate: Mechanism, Kinetics and Implication for *in situ* Chemical Oxidation

Huabin Zeng [a], Xu Zhao [b], Feiping Zhao [a, e*], Yuri Park [a], Eveliina Repo [a], Senthil K. Thangaraj [c], Janne Jänis [c], Mika Sillanpää [d]

[a] Department of Separation Science, LUT University, Sammonkatu 12, FI-50130 Mikkeli, Finland

[b] State Key Laboratory of Environmental Aquatic Chemistry, Research Center for Eco-Environmental Sciences, Chinese Academy of Sciences, Beijing 100085, China

[c] Department of Chemistry, University of Eastern Finland, P.O. Box 111, FI-80101 Joensuu, Finland

[d] Department of Civil and Environmental Engineering, Florida International University, Miami, USA

e Institute of Environmental Engineering, School of Metallurgy and Environment, Central South University, Changsha, 410083, China

*Corresponding author:

Department of Separation Science

Lappeenranta-Lahti University of Technology LUT

Sammonkatu 12, FI-50130 Mikkeli, Finland

e-mail address: Feiping.Zhao@lut.fi; Feiping.zhao@csu.edu.cn

Table of Contents/Graphic Abstract

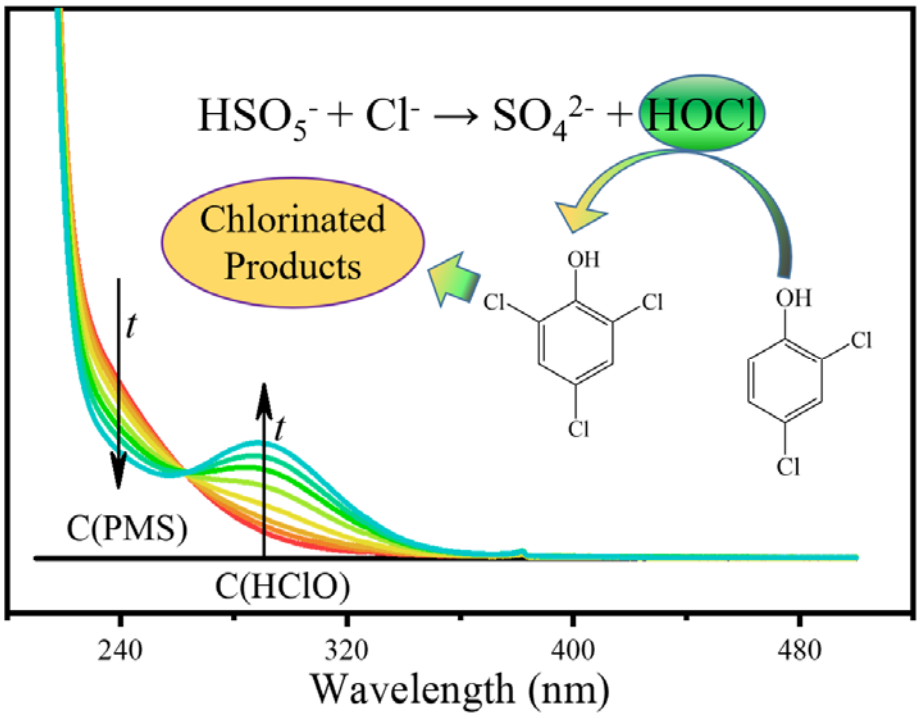

Abstract

Inorganic and organic pollutants present a hazard to surface and groundwater resources. Peroxymonosulfate (PMS, HSO_5^-) has received increasing attention for *in situ* chemical oxidation (ISCO) capable of remediating contaminated sites. Considering that saline waters occur widely in natural environments, it is desirable to evaluate the effect of Cl^- on the PMS oxidation of organic compounds. In this study, 2,4-dichlorophenol (2,4-DCP) was used as a model pollutant. At a PMS concentration of 2.0 mM, Cl^- concentration of 50 mM, and solution pH of 7.0, 2,4-DCP was completely degraded by PMS in the presence of Cl^- (PMS/Cl^- system), while PMS alone exhibited almost no reactivity with 2,4-DCP. The degradation of 2,4-DCP was optimized at a solution pH of 8.4 and high concentrations of PMS and Cl^-. Quenching experiments and degradation pathway analyses indicated that HClO was responsible for 2,4-DCP oxidation, and HClO was mainly generated by the interaction of Cl^- with HSO_5^-, rather than SO_5^{2-}. Consequently, the transformation from HSO_5^- to HClO appeared under a solution pH of 10.0 and was favored in an acidic solution. Given the ambient pH and Cl^- concentrations of saline waters, a considerable amount of HClO may be produced by the interaction of PMS with Cl^- in the oxidant delivery stage of ISCO processes. Interestingly, H_2O_2 and peroxydisulfate did not exhibit reactions similar to those of PMS. This research indicated that caution must be exercised when choosing an oxidant for ISCO processes in saline waters.

Keywords: 2,4-Dichlorophenol, peroxymonosulfate, Cl^-, hypochlorous acid, *in situ* chemical oxidation

1. Introduction

In the past few decades, ground and surface water has seen considerable contamination with organic and inorganic pollutants, which are raising concerns because of their ubiquitous presence, recalcitrance in the environment, and toxicity to humans and wildlife (Liu and Wong, 2013; Tsitonaki et al., 2010). According to recent studies at both the laboratory and pilot scales, *in situ* chemical oxidation (ISCO) has been proven to be instrumental in remediating contaminated areas (Devi et al., 2016; Tsitonaki et al., 2010). Generally, the oxidants in an ISCO process must be stable during oxidant delivery to the targeted area and highly reactive in the contaminated zone (Yuan et al., 2014). Peroxymonosulfate (PMS), which is a promising oxidant, presents weak self-decomposition at circumneutral pH levels (Yang et al., 2018); when initiated by an activator, PMS can produce sulfate ($SO_4^{\cdot-}$) and hydroxyl (·OH) radicals that can destroy a wide range of toxic organic compounds (Ghanbari and Moradi, 2017). Some organic pollutants, such as ketones, benzoquinone, phenols and steroid estrogens, can be degraded by PMS without an activator (Montgomery, 1974; Zhou et al., 2015; Zhou et al., 2018b; Zhou et al., 2017). These properties make PMS a promising oxidant for ISCO technologies, as it minimizes losses during oxidant delivery to the targeted area and exhibits strong oxidation capacity under the influence of additional catalysts or the pollutants themselves, in the contaminated zone.

A critical issue that must be carefully considered in ISCO studies of natural waters is the complexity of the water matrices, especially those containing Cl^-; for example, seawater contains high concentrations of salts (up to 35‰), that typically include NaCl, $MgCl_2$, and $CaCl_2$. Moreover, Cl^- is also ubiquitous in surface waters; according to previous statistical analyses, water in saline lakes accounts for half of the surface water on Earth (Vallentyne, 1972). The concentration of Cl^- is also relatively high even in groundwater; for example, its concentration was determined to range

from 10–3000 ppm in California (Mendenhall et al., 1916). Given the ubiquity of Cl^- in natural waters, its impacts are nonnegligible when PMS is used for water treatment and environmental rehabilitation.

This study investigates the interactions of Cl^- and activated PMS, as well as subsequent oxidation processes. Cl^- is highly reactive to sulfate and hydroxyl radicals, causing the following series of reactions (**reactions 1–4**) (Anipsitakis et al., 2006; Grebel et al., 2010):

$$SO_4^{\cdot-} + Cl^- \leftrightarrow SO_4^{2-} + Cl\cdot \quad (1)$$

$$\cdot OH + Cl^- \leftrightarrow OH^- + Cl\cdot \quad (2)$$

$$Cl\cdot + Cl^- \leftrightarrow Cl_2^{\cdot-} \quad (3)$$

$$2Cl_2^{\cdot-} \leftrightarrow Cl_2 + 2Cl^-. \quad (4)$$

From the perspective of degradation kinetics, the presence of Cl^- in an activated PMS system has differing influences on different organic compounds. For example, Cl^- has almost no influence on the degradation kinetics of monochlorophenols and 3-cyclohexene-1-carboxylic acid (Fang et al., 2017; Yang et al., 2014). However, Cl^- adversely affects the oxidation efficiency of activated PMS for benzoic acid, cyclohexanecarboxylic acid, and atrazine (Chan and Chu, 2009; Yang et al., 2014), while accelerating the degradation of phenolic compounds and the decolorization of azo dye (Acid Orange #7) (Anipsitakis et al., 2006; Yang et al., 2010). Despite these differences in behavior, all these phenomena depend upon whether or not the rate constants of organics with $Cl\cdot$, $Cl_2^{\cdot-}$, and Cl_2 are higher than those with sulfate and hydroxyl radicals (Yang et al., 2014). Furthermore, Wang et al. (2011) and Zhou et. al (2018b) proposed that the production of active chlorine from the reaction of unactivated PMS with Cl^- could be used as an enhanced regime degrade Acid Orange #7 degradation and oxidize steroid estrogen (**reaction 5**). Furthermore, PMS readily counters the effects of various fungi and bacteria in saline waters (Delcomyn et al., 2006;

Wen et al., 2019). These studies reveal the use of PMS in the operando remediation of saline waters, even without an activator. To evaluate the application potential of PMS to ISCO, it is necessary to investigate the dominant oxidative mechanism and quantify the importance of this mechanism within the time scale, solution pH range and Cl^- content relevant to ISCO processes.

$$HSO_5^- + Cl^- \rightarrow HClO + SO_4^{2-} \quad (5)$$

In this study, 2,4-dichlorophenol (2,4-DCP) was used as a model contaminant, not only because of its relevance as a contaminant in surface waters and groundwater but also due to its interaction with reactive oxygen species (ROS), including hydroxyl and sulfate radicals, singlet oxygen ($^1O_2$), and chlorine (**Table S-1**) (Chen et al., 2016; Cheng et al., 2017; Gallard and Von Gunten, 2002; Gan et al., 2018). The ROS in the PMS/Cl^- system was determined by ultraviolet-visible (UV-vis) spectral analyses, quenching experiments, and degradation product analysis. The performance characteristics of the PMS/Cl^- system at various solution pH levels were also evaluated and kinetic analyses were utilized to quantify the impact of Cl^- on ISCO technologies involving PMS. Finally, the value of utilizing PMS in ISCO processes was explored.

2. Materials and Methods

2.1 Chemicals

For this study, 2,4-DCP, PMS ($KHSO_5^-$, available as Oxone® ($KHSO_5 \cdot 0.5KHSO_4 \cdot 0.5K_2SO_4$)), sodium peroxydisulfate (PDS), hydrogen peroxide (H_2O_2), sodium hypochlorite solution (NaClO), sodium chloride (NaCl), sodium sulfide (Na_2SO_4), sodium sulfite (Na_2SO_3), sodium phosphate monobasic (NaH_2PO_4), sodium phosphate dibasic (Na_2HPO_4), sodium phosphate tribasic dodecahydrate ($Na_3PO_4 \cdot 12H_2O$), dimethyl pyridine N-oxide (DMPO), and 2,2,6,6-tetramethyl-4-piperidone (TEMP) were purchased from the Sigma-Aldrich Corporation (USA).

2.2 Experimental Setup

All solutions in this study were prepared using deionized water (resistivity: 18.2 MΩ) from an arium® pro system (Sartorius AG, Germany). The solution pH was regulated using either 100 mM of NaOH or 50 mM of H_2SO_4. Simulated saline water was prepared using NaCl and experiments were conducted in 150-mL reagent bottles. To quench the oxidant and stop 2,4-DCP degradation, Na_2SO_3 solution was added to the samples taken from the reactor.

2.3 Analytical Methods

The concentration of 2,4-DCP was determined by high-performance liquid chromatography (HPLC, LC-20AD, Shimadzu Corp., Japan) with a C18 column, column temperature of 35℃, and ultraviolet detector wavelength of 284 nm. The mobile phase was maintained at a flow rate of 1.0 mL/min with a constant volumetric ratio of methanol and water (70/30). The HClO and PMS concentrations were measured with an UV-vis spectrophotometer (Lambda 45, PerkinElmer, Inc., USA); the specific calculation methods are shown in the Supporting Information (**Text SI-2, Text SI-3**).

ROS were identified using an electron spin resonance (ESR) spectrometer (CMS 8400, Adani Systems, USA). The samples were collected from the reaction solution at different times and DMPO was used to capture ·OH and $SO_4^{\cdot-}$ by forming DMPO-OH and DMPO-SO_4 adducts, while TEMP was employed in $^1O_2$ measurements. The intermediates and byproducts of 2,4-DCP degradation were identified using high-resolution quadrupole time-of-flight mass spectrometry (QTOF-MS), for which 2,4-DCP samples (20 μL) were diluted with 180 μL of acetonitrile (HPLC-grade) for direct infusion measurements. All measurements were conducted using a Bruker time-of-flight (TOF) instrument (Bruker Daltonics, Germany) coupled with an electrospray ionization (ESI) source (Apollo-II, Bruker Daltonics, Germany) operated in negative-ion mode. Samples were injected at a flow rate of 2 μL/min. Dry nitrogen was used as a drying agent (80°C, 4.0 L/min)

and nebulizing gas (1.0 bar). An electrospray (ES) tuning calibration mixture was employed to calibrate mass spectra (Agilent Technologies, USA). Chloroform and chlorinated acetic acid were analyzed by using a gas chromatography–Mass spectrometry (GC-MS, Thermo) (**Text SI-4**).

3. Results and discussion

3.1 PMS oxidation for 2,4-DCP degradation

First, the 2,4-DCP was degraded by 2.0 mM of PMS in the absence of Cl^-. As shown in **Figure 1**, only 2.56% of the 2,4-DCP was degraded by unactivated PMS (2.0 mM) with a solution pH of 7.0 after 60 min, which indicates that PMS alone is not very reactive to 2,4-DCP. The slight reduction in 2,4-DCP might have been due to oxidation by $^1O_2$ from the self-decomposition of PMS (Cheng et al., 2017; Yang et al., 2018) or PMS activation by phosphate buffer in this study. We then investigated the performance of the PMS system for 2,4-DCP degradation in saline water. With the addition of 50 mM of Cl^-, complete decomposition of 2,4-DCP was achieved within 60 min. These results agree with results of other studies (Anipsitakis et al., 2008; Zhou et al., 2018b) that suggest that Cl^- is important to organic degradation in the PMS/Cl^- process.

3.2 ROS detection

ESR spectroscopy with a spin-trapping reagent of either DMPO or TEMP was used to directly identify the radicals in the PMS/Cl^- process under various solution pH levels. However, no DMPO-SO_4 or DMPO-OH signals were observed in the PMS/Cl^- system, which ruled out the possibility of $SO_4^{\cdot-}$ and ·OH being the main ROS. Surprisingly, a three-line ESR spectrum with equal intensities was detected, suggesting the generation of $^1O_2$ in the PMS/Cl^- system at all pH levels (**Figure SI-4**) (Cheng et al., 2017). Theoretically, $^1O_2$ can be produced from the self-decomposition and alkaline activation of PMS (Qi et al., 2016; Yang et al., 2018). Here, we studied the 2,4-DCP oxidation by PMS alone at various pH levels (5.0~11.5) and found that degradation efficiencies at

all pH levels were confined to no more than 4% in 60 min (**Text SI-5**). $^1O_2$ appears to have played an insignificant role in 2,4-DCP degradation in the PMS/Cl^- process given the low alkalinity and high salinity in this study.

According to thermodynamics, it is theoretically feasible to convert PMS (1.75 V) to available chlorine species (1.48 V HClO/Cl^-) via **reaction 6** as follows (Anipsitakis et al., 2006).

$$PMS + Cl^- \rightarrow K^+ + SO_4^{2-} + HClO \quad (6)$$

To assess the emergence of HClO, the UV-vis spectra of the PMS/Cl^- reaction solution in the absence of 2,4-DCP were recorded at different times. Compared to the UV-vis spectrum of the pure phosphate buffer, two absorption peaks appeared at wavelengths of 240 nm and 293 nm, which were assigned to the absorption of the PMS and HClO (**Figure 2a**), respectively. As time proceeded, the signal intensity at a wavelength of 293 nm increased, while that at 240 nm decreased simultaneously, implying that PMS was the precursor of the produced HClO.

Herein, quenching experiments were conducted to further analyze the importance of HClO to 2,4-DCP degradation in the PMS/Cl^- process. We chose $(NH_4)_2SO_4$ with a solution pH of 8.9 as the quenching agent for HClO because NH_3, an existing species in an $(NH_4)_2SO_4$ solution, is highly reactive to HClO but inert to PMS (Heeb et al., 2017). As shown in **Figure 2b**, the degradation of 2,4-DCP was significantly inhibited in the presence of $(NH_4)_2SO_4$. More specifically, the degradation efficiencies of 2,4-DCP were only 31.21% and 13.11%, respectively, in the presence of 0.5 mM and 1.0 mM of $(NH_4)_2SO_4$; when the $(NH_4)_2SO_4$ concentration was further increased to 5.0 and 10.0 mM, the degradation of 2,4-DCP was completely inhibited. Although NH_4^+ reacts with both hydroxyl and sulfate radicals (Deng and Ezyske, 2011; Neta et al., 1988), ESR analyses confirmed that such radicals are nonexistent in the PMS/Cl^- process, thus demonstrating that the HClO generated in the PMS/Cl^- process is mainly responsible for 2,4-DCP degradation.

3.3 Effect of solution pH

The effect of solution pH on the degradation of 2,4-DCP in the PMS/Cl^- process was investigated, and the results are shown in **Figure 3**. At a pH of 11.5, 2,4-DCP degradation was not observed. As the pH decreased to 8.4 and 7.6, the degradation efficiencies at 30 min increased to 94.62% and 98.23%, respectively. Interestingly, with a further decrease in pH, 2,4-DCP degradation actually declined.

To clarify the unintuitive trend of 2,4-DCP degradation at various solution pH levels in the PMS/Cl^- process, we investigated the effect of pH on HClO production in the absence of 2,4-DCP (**Figure SI-6**). As PMS consumption is stoichiometrically equal to the generation of HClO in **reaction 6**, we used the PMS consumption process as a substitute for the HClO production process to determine the kinetic properties of the PMS/Cl^- system. The kinetic constants of PMS consumption using a first-order reaction rate are shown in **Figure 4a**. At pH levels greater than 10.4, no HClO generation was observed; however, the transformation of PMS to HClO accelerated when the pH was reduced from 10.4 to 7.0 (0.00143 min^{-1}, R^2=0.9994). At a pH of 7.0, the kinetic constant was maximized, and a further decrease in the solution pH no longer influenced this constant.

The distribution of HSO_5^- and SO_5^{2-} species at various solution pH levels could be obtained mathematically based on the pKa of HSO_5^- (9.4) (Ball and Edwards, 1956) (**Figure 4a, Text SI-6**). Comparing the curves of these two reveals that variations of the kinetic constants as a function of solution pH were highly consistent with the trends of HSO_5^- ion percentages as a function of pH (Yang et al., 2018). These results also demonstrate that the HClO was produced mainly from the interaction of Cl^- with HSO_5^- ions via **reaction 5**. According to Lente et al. (2009), SO_5^{2-} is far less reactive to Cl^- compared to HSO_5^-.

Generally, 2,4-DCP degradation is influenced by the HClO production rate and by the properties of 2,4-DCP oxidation by HClO. The HClO produced may be converted to less oxidative ClO^- in alkaline solutions (**Figure 4b, Figure SI-7**) (Gallard and Von Gunten, 2002). Moreover, 2,4-DCP formed in two species (pKa=7.85), depending on the solution pH, including 2,4-dichlorphenol molecules (protonated 2,4-DCP) and 2,4-dichlorphenolic ions (deprotonated 2,4-DCP, 2,4-DCP ion) (Lee and Morris, 1962). The different 2,4-DCP species show different reactivities to HClO. Normally, the rate constants for the reaction of HClO with deprotonated phenolic compounds are 3–5 orders of magnitude higher than those for reactions with protonated phenolic compounds (Gallard and Von Gunten, 2002; Ge et al., 2006). As the solution pH decreases, the percentage of deprotonated 2,4-DCP also decreases (**Figure 4b**, **Figure SI-8**) (Wagner and Schulz, 2001). 2,4-DCP degradation (pseudo-first order kinetic constants) was influenced by HClO production and the percentage of HClO and deprotonated 2,4-DCP in the PMS/Cl^- system and thus exhibited a similar tendency to the production of HSO_5^-, HClO, and deprotonated 2,4-DCP percentages as a function of pH (**Figure 4b**). Consequently, the pH-dependent process reached the maximum degradation rate at a pH of 7.6 in the PMS/Cl^- system.

3.4 Kinetics

Figure 5a shows the variations in the 2,4-DCP degradation efficiency as a function of the Cl^- concentration in the solution. Increasing the Cl^- concentration significantly enhanced the removal of 2,4-DCP. The degradation efficiency within 60 min was 26.64% at a Cl^- concentration of 5 mM; when the concentration of Cl^- increased from 5 to 50 mM and 100 mM, the 2,4-DCP was completely degraded in only 45 min and 30 min, respectively.

As illustrated by **reaction 5**, Cl^- is among the reactants that produce HClO in the PMS/Cl^- process. Since 2,4-DCP itself cannot be directly oxidized by Cl^- and the kinetic constant between HClO

and 2,4-DCP is up to 303 $M^{-1}\cdot s^{-1}$ (Gallard and Von Gunten, 2002), the Cl^- affects the 2,4-DCP degradation processes via HClO as an intermediate product. **Figure 5b**, which shows the variations in the UV-vis spectra of the PMS/Cl^- reaction solution over 120 min for various Cl^- concentrations, verifies this supposition. The increasing intensity at a wavelength of 293 nm further indicates that HClO production was accelerated by a high concentration of Cl^-, which enhanced the 2,4-DCP degradation process.

Similar results were seen in the effect of PMS dosage, another reactant in reaction 5. **Figures 5c** and **5d** illustrate the effect of the PMS dosage on 2,4-DCP degradation and on the production of HClO. It is obvious that PMS at higher concentrations promoted its conversion from PMS to HClO (**Figure 5d**). A higher concentration of HClO as a ROS also led to a higher rate of 2,4-DCP degradation.

The kinetic constant of the transformation from HSO_5^- to HClO was estimated at a solution pH of 7.0 and a temperature of 298 ℃. Here, PMS mainly existed as HSO_5^-. Usually, the reaction rate in a binary reaction can be expressed by **equation a**. In our kinetic experiments, $C(Cl^-)$ can be regarded as a constant because its consumption is less than 1%. The results in **Figure 6a** illustrate that PMS consumption was well fitted by a pseudo-first-order reaction model at each given Cl^- concentration. Based on **equations b** to **e**, k_{obs} should be equal to $k\cdot C(Cl^-)$. As shown in **Figure 6a** (inset), plotting k_{obs} vs $C(Cl^-)$ yielded a linear curve with a slope of approximately 0.0005 $M^{-1}s^{-1}$ and a correlation coefficient of 0.994.

$$v = \frac{dC(HSO_5^-)}{dt} = -k \cdot C(Cl^-) \cdot C(HSO_5^-) \quad \text{(a)}$$

$$\frac{1}{C(HSO_5^-)} dC(HSO_5^-) = -k \cdot C(Cl^-)dt \quad \text{(b)}$$

$$\int_0^t \frac{1}{C(HSO_5^-)} dC(HSO_5^-) = \int_0^t -k \cdot C(Cl^-)dt \quad \text{(c)}$$

$$\ln \frac{C_t(HSO_5^-)}{C_0(HSO_5^-)} = -k \cdot C(Cl^-) \cdot t = -k_{obs} \cdot t \quad \text{(d)}$$

$$k_{obs} = k \cdot C(Cl^-) \quad \text{(e)}$$

$$v(HClO) = -v(HSO_5^-) = (0.0005\ M^{-1}s^{-1}) \cdot C(Cl^-) \cdot C(HSO_5^-) \quad \text{(f)}$$

The value of 0.0005 $M^{-1}s^{-1}$ was further confirmed by varying the concentration of PMS and fixing the Cl^- concentration (50 mM). As shown in **Figure 6b**, the decomposition ratios of PMS were maintained at almost the same values throughout the process. In this way, the value of *k* could be calculated as (0.000486 ± 0.000048) $M^{-1}s^{-1}$, which is nearly equal to 0.0005 $M^{-1}s^{-1}$.

3.5 Degradation pathway analysis

The degradation of 2,4-DCP in the PMS/Cl^- system was further explored using ESI-QTOF-MS. To identify intermediates, a high 2,4-DCP concentration (500 μM) was applied. The concentration of PMS was maintained at 20 times the 2,4-DCP concentration, while the Cl^- concentration was held at 50 mM. As shown in **Figure SI-9**, after 10 min of reaction time, the signal for the 2,4-DCP (*m/z* 160.95 for the $[M–H]^-$ ion) decreased while some new signals at m/z 194.91, 196.90, 198.90, and 200.90 appeared at an intensity ratio of 27:27:9:1. This finding suggests the formation of 2,4,6-trichlorophenol (2,4,6-TCP), which clearly increased over time. Similar results occurred in the GC-MS analysis of treated 2,4-DCP sample (**Text SI-4**). Additionally, a minor signal was observed at *m/z* 176.89, which is consistent with a dichlorinated hydroquinone, either 3,5-dichloro-1,2-hydroquinone or 2,4-dichloro-1,5-hydroquinone. With further oxidation of intermediates, some small degradation products were determined by GC-MS analysis, including chloroform and Monochloroacetic acid (**Text SI-4**). Based on these results, we proposed that the main pathway of 2,4-DCP degradation was via formation of 2,4,6-TCP followed by ring-opening reactions and subsequent decomposition to chloroform, chloroacetic acid (**Figure 7**), H_2O and CO_2 (**Text SI-7**) (Xu and Wang, 2012).

The oxidation of 2,4-DCP driven by different reactive species presented different degradation routes. As shown in **Table SI-2**, various chloro-hydroquinone and chloro-benzoquinone were

formed from ·OH oxidation (Chu et al., 2005; Kang et al., 2002), $SO_4^{\cdot-}$ oxidation (Huie et al., 1991; Zhou et al., 2018a), and non-radical oxidation of 2,4-DCP (Zhang et al., 2014). Comparing these degradation pathways with that in the PMS/Cl^- system, especially the emergence of 2,4,6-TCP as a major intermediate species, unravels another oxidation mechanism and a different intermediate oxidant. It has also been reported that 2,4,6-TCP is a feature of the 2,4-DCP chlorination process in which HClO is the main oxidation species (Deborde and von Gunten, 2008). **Figure SI-9** makes clear that 2,4,6-TCP appeared as the 2.4-DCP concentration decreased over time in a pure chlorination system. The degradation consistency of these two systems reveals that the PMS/Cl^- system is primarily a chlorination process in terms of its oxidation mechanism.

3.6 Implications for ISCO

Generally, ISCO processes are divided into two phases: oxidant delivery and remediation (Chowdhury et al., 2017). Several studies have addressed the radical oxidation processes for PMS-related oxidation reactions in remediation stage, whereas few have highlighted the interactions of unactivated PMS with other environmental impurities in delivery phase (Ghanbari and Moradi, 2017). According to previous research, it may take several days for the oxidants to cover the entirety of the target area, while it may even take one month in some low-permeability zones (Chowdhury et al., 2017). Our kinetics study suggests that a considerable amount of HClO may be generated from the interaction of PMS with Cl^- at the time scale of the delivery stage (several days). Contaminated areas, in particular, provide favorable conditions for the transformation of PMS to HClO. For example, Cl^- concentrations higher than 5 mM and pH levels below 10.0 occur widely in natural aqueous environments (Mendenhall et al., 1916), thereby increasing the likelihood of HClO production via methods demonstrated in this study. The HClO produced in the delivery stage may induce some unexpected reactions in the subsequent remediation stage of ISCO,

which brings advantages and disadvantages for the ISCO process. Unactivated PMS is relatively inert to most contaminants (Ghanbari and Moradi, 2017). Thus, the *in-situ* transformation of PMS to HClO can significantly reduce the demand for PMS activators while simultaneously preventing secondary pollution induced by the latter. Furthermore, HClO shows a high reactivity with organics with particular components, such as reduced sulfur moieties, amines, and activated aromatic systems (Heeb et al., 2017), and can degrade these quickly. The disinfection performance of PMS will be enhanced in the presence of Cl^- because of the good performance of HClO in inactivating pathogenic microorganisms (Wen et al., 2019). However, the indirect oxidation of PMS via HClO production may hinder the desired goal of eliminating hazards if the degradation is routed through pathways that lead to the production of other toxic and carcinogenic chlorination byproducts (Bull et al., 1995).

Interestingly, H_2O_2 and PDS share the same structure with PMS (a peroxy bond) (Ghanbari and Moradi, 2017), but neither H_2O_2 nor PDS oxidation was observed to degrade 2,4-DCP in the presence of Cl^- (**Figure SI-10**). This finding indicates that either that H_2O_2 and PDS do not react with Cl^- in a manner similar to the way PMS does or that the kinetics are too slow to allow for the observation of active chlorine generation. From this perspective, H_2O_2 and PDS may be better substitutes for PMS if chlorination is not desired. Together, these findings can provide guidance for choosing a suitable oxidant for the ISCO process.

4. Conclusion

The synergetic effect of Cl^- and PMS on the degradation of 2,4-DCP was investigated in detail, and the potential of applying PMS in the ISCO process of contaminated saline waters was evaluated. Our results showed that at a PMS concentration of 2.0 mM, Cl^- concentration of 50 mM, and solution pH of 7.0, 2,4-DCP was completely degraded in the PMS/Cl^- system, while PMS

alone displayed almost no reactivity. Optimal parameters for 2,4-DCP removal included a solution pH of 8.5 and high concentrations of PMS and Cl^-. Efficient 2,4-DCP degradation can be ascribed to the generation of HClO from PMS and Cl^-. Furthermore, UV-vis spectra and quenching experiments confirmed that HClO is the main oxidation species in the PMS/Cl^- system. The emergence of 2,4,6-TCP, which is a symbolic product of 2,4-DCP chlorination, in the degradation pathway further verified this conclusion. Hypochlorous acid was mainly generated from the interaction of Cl^- with HSO_5^-, rather than SO_5^{2-}. Consequently, the transformation from HSO_5^- to HClO appeared under a solution pH of 10.0 and was favored in an acidic solution. Its generation rate can be expressed as $v(HClO)=(0.0005\ M^{-1}s^{-1})\cdot C(Cl^-)\cdot C(HSO_5^-)$. Given the ambient pH and Cl^- concentration of saline waters, a considerable amount of HClO may be produced from the interaction of PMS with Cl^- in the oxidant delivery phase of ISCO processes. Moreover, H_2O_2 and peroxydisulfate showed no reactions that were similar to those of PMS. These findings suggest that extreme care must be taken when choosing an oxidant for ISCO processes in saline waters.

Acknowledgements

The authors are grateful to the Academy of Finland and the European Union for funding this project. The FT-ICR MS facility is supported by Biocenter Finland/Biocenter Kuopio and the European Regional Development Fund (Grant A70135).

Supporting information

7 sections of Text, 10 Figures and 2 Table are attached.

References

321 Anipsitakis GP, Dionysiou DD, Gonzalez MA. Cobalt-mediated activation of peroxymonosulfate
322 and sulfate radical attack on phenolic compounds. Implications of chloride ions.
323 Environmental Science & Technology 2006; 40: 1000-1007.
324 Anipsitakis GP, Tufano TP, Dionysiou DD. Chemical and microbial decontamination of pool
325 water using activated potassium peroxymonosulfate. Water Research 2008; 42: 2899-2910.
326 Ball DL, Edwards JO. The kinetics and mechanism of the decomposition of Caro's acid. I. Journal
327 of the American Chemical Society 1956; 78: 1125-1129.
328 Bull RJ, Birnbaum LS, Cantor KP, Rose JB, Butterworth BE, Pegram R, et al. Water chlorination:
329 Essential process or cancer hazard? Fundamental and Applied Toxicology 1995; 28: 155-
330 166.
331 Chan KH, Chu W. Degradation of atrazine by cobalt-mediated activation of peroxymonosulfate:
332 Different cobalt counteranions in homogenous process and cobalt oxide catalysts in
333 photolytic heterogeneous process. Water Research 2009; 43: 2513-2521.
334 Chen JX, Gao NY, Lu X, Xia M, Gu ZC, Jiang C, et al. Degradation of 2,4-dichlorophenol from
335 aqueous using UV activated persulfate: kinetic and toxicity investigation. RSC Advances
336 2016; 6: 100056-100062.
337 Cheng X, Guo HG, Zhang YL, Wu X, Liu Y. Non-photochemical production of singlet oxygen
338 via activation of persulfate by carbon nanotubes. Water Research 2017; 113: 80-88.
339 Chowdhury AIA, Gerhard JI, Reynolds D, O'Carroll DM. Low permeability zone remediation via
340 oxidant delivered by electrokinetics and activated by electrical resistance heating: proof of
341 concept. Environmental Science & Technology 2017; 51: 13295-13303.

342 Chu W, Kwan CY, Chan KH, Kam SK. A study of kinetic modelling and reaction pathway of 2,4-
343 dichlorophenol transformation by photo-fenton-like oxidation. Journal of Hazardous
344 Materials 2005; 121: 119-126.
345 Deborde M, von Gunten U. Reactions of chlorine with inorganic and organic compounds during
346 water treatment - Kinetics and mechanisms: A critical review. Water Research 2008; 42:
347 13-51.
348 Delcomyn CA, Bushway KE, Henley MV. Inactivation of biological agents using neutral oxone-
349 chloride solutions. Environmental Science & Technology 2006; 40: 2759-2764.
350 Deng Y, Ezyske CM. Sulfate radical-advanced oxidation process (SR-AOP) for simultaneous
351 removal of refractory organic contaminants and ammonia in landfill leachate. Water
352 Research 2011; 45: 6189-6194.
353 Devi P, Das U, Dalai AK. In-situ chemical oxidation: Principle and applications of peroxide and
354 persulfate treatments in wastewater systems. Science of the Total Environment 2016; 571:
355 643-657.
356 Fang CL, Lou XY, Huang Y, Feng M, Wang ZH, Liu JS. Monochlorophenols degradation by
357 UV/persulfate is immune to the presence of chloride: Illusion or reality? Chemical
358 Engineering Journal 2017; 323: 124-133.
359 Gallard H, Von Gunten U. Chlorination of phenols: Kinetics and formation of chloroform.
360 Environmental Science & Technology 2002; 36: 884-890.
361 Gan L, Li BB, Guo MY, Weng XL, Wang T, Chen ZL. Mechanism for removing 2,4-
362 dichlorophenol via adsorption and Fenton-like oxidation using iron-based nanoparticles.
363 Chemosphere 2018; 206: 168-174.

364 Ge F, Zhu LZ, Chen HR. Effects of pH on the chlorination process of phenols in drinking water.
365 Journal of Hazardous Materials 2006; 133: 99-105.
366 Ghanbari F, Moradi M. Application of peroxymonosulfate and its activation methods for
367 degradation of environmental organic pollutants: Review. Chemical Engineering Journal
368 2017; 310: 41-62.
369 Grebel JE, Pignatello JJ, Mitch WA. Effect of halide ions and carbonates on organic contaminant
370 degradation by hydroxyl radical-based advanced oxidation processes in saline waters.
371 Environmental Science & Technology 2010; 44: 6822-6828.
372 Heeb MB, Kristiana I, Trogolo D, Arey JS, von Gunten U. Formation and reactivity of inorganic
373 and organic chloramines and bromamines during oxidative water treatment. Water
374 Research. 2017; 110; 91-101.
375 Huie RE, Clifton CL, Kafafi SA. Rate constants for hydrogen abstraction reactions of sulfate
376 radical, $SO_4^{\cdot-}$ experimental and theoretical results for cyclic ethers. Journal of Physical
377 Chemistry 1991; 95: 9336-9340.
378 Kang N, Lee DS, Yoon J. Kinetic modeling of Fenton oxidation of phenol and monochlorophenols.
379 Chemosphere 2002; 47: 915-924.
380 Lee GF, Morris JC. Kinetics of chlorination of phenol-chlorophenolic tastes and odors. Int. J. Air
381 Water Pollut 1962; 6: 419-431.
382 Lente G, Kalmar J, Baranyai Z, Kun A, Kek I, Bajusz D, et al. One- versus two-electron oxidation
383 with peroxomonosulfate ion: reactions with iron(II), vanadium(IV), halide Ions, and
384 photoreaction with cerium(III). Inorganic Chemistry 2009; 48: 1763-1773.
385 Liu JL, Wong MH. Pharmaceuticals and personal care products (PPCPs): A review on
386 environmental contamination in China. Environment International 2013; 59: 208-224.

387 Mendenhall WC, Dole RB, Stabler H. Ground water in San Joaquin Valley, California. Govt. Print.
388 Off., 1916.
389 Montgomery RE. Catalysis of peroxymonosulfate reactions by ketones. Journal of the American
390 Chemical Society 1974; 96: 7820-7821.
391 Neta P, Huie RE, Ross AB. Rate constants for reactions of inorganic radicals in aqueous-solution.
392 Journal of Physical and Chemical Reference Data 1988; 17: 1027-1284.
393 Qi CD, Liu XT, Ma J, Lin CY, Li XW, Zhang HJ. Activation of peroxymonosulfate by base:
394 Implications for the degradation of organic pollutants. Chemosphere 2016; 151: 280-288.
395 Tsitonaki A, Petri B, Crimi M, Mosbaek H, Siegrist RL, Bjerg PL. In situ chemical oxidation of
396 contaminated soil and groundwater using persulfate: A review. Critical Reviews in
397 Environmental Science and Technology 2010; 40: 55-91.
398 Vallentyne JR. Freshwater supplies and pollution: Effects of the demophoric explosion on water
399 and man. The Environmental Future 1972: 181-211.
400 Wagner K, Schulz S. Adsorption of phenol, chlorophenols, and dihydroxybenzenes onto
401 unfunctionalized polymeric resins at temperatures from 294.15 K to 318.15 K. Journal of
402 Chemical and Engineering Data 2001; 46: 322-330.
403 Wang P, Yang SY, Shan L, Niu R, Sha XT. Involvements of chloride ion in decolorization of Acid
404 Orange 7 by activated peroxydisulfate or peroxymonosulfate oxidation. Journal of
405 Environmental Sciences 2011; 23: 1799-1807.
406 Wen G, Zhao D, Xu XQ, Chen ZH, Huang TL, Ma J. Inactivation of fungi from four typical genera
407 in groundwater using PMS/Cl- system: Efficacy, kinetics and mechanisms. Chemical
408 Engineering Journal 2019; 357: 567-578.

409 Xu LJ, Wang JL. Fenton-like degradation of 2,4-dichlorophenol using Fe3O4 magnetic
410 nanoparticles. Applied Catalysis B: Environmental 2012; 123: 117-126.
411 Yang SY, Wang P, Yang X, Shan L, Zhang WY, Shao XT, et al. Degradation efficiencies of azo
412 dye Acid Orange 7 by the interaction of heat, UV and anions with common oxidants:
413 Persulfate, peroxymonosulfate and hydrogen peroxide. Journal of Hazardous Materials
414 2010; 179: 552-558.
415 Yang Y, Banerjee G, Brudvig GW, Kim JH, Pignatello JJ. Oxidation of organic compounds in
416 water by unactivated peroxymonosulfate. Environmental Science & Technology 2018; 52:
417 5911-5919.
418 Yang Y, Pignatello JJ, Ma J, Mitch WA. Comparison of halide impacts on the efficiency of
419 contaminant degradation by sulfate and hydroxyl radical-based advanced oxidation
420 processes (AOPs). Environmental Science & Technology 2014; 48: 2344-2351.
421 Yuan SH, Liao P, Alshawabkeh AN. Electrolytic manipulation of persulfate reactivity by iron
422 electrodes for trichloroethylene degradation in groundwater. Environmental Science &
423 Technology 2014; 48: 656-663.
424 Zhang T, Chen Y, Wang Y, Le Roux J, Yang Y, Croué J-P. Efficient peroxydisulfate activation
425 process not relying on sulfate radical generation for water pollutant degradation.
426 Environmental science & technology 2014; 48: 5868-5875.
427 Zhou P, Zhang J, Zhang YL, Zhang GC, Li WS, Wei CM, et al. Degradation of 2,4-dichlorophenol
428 by activating persulfate and peroxomonosulfate using micron or nanoscale zero-valent
429 copper. Journal of Hazardous Materials 2018a; 344: 1209-1219.

Zhou Y, Jiang J, Gao Y, Ma J, Pang SY, Li J, et al. Activation of peroxymonosulfate by benzoquinone: A novel nonradical oxidation process. Environmental Science & Technology 2015; 49: 12941-12950.

Zhou Y, Jiang J, Gao Y, Pang SY, Ma J, Duan JB, et al. Oxidation of steroid estrogens by peroxymonosulfate (PMS) and effect of bromide and chloride ions: Kinetics, products, and modeling. Water Research 2018b; 138: 56-66.

Zhou Y, Jiang J, Gao Y, Pang SY, Yang Y, Ma J, et al. Activation of peroxymonosulfate by phenols: Important role of quinone intermediates and involvement of singlet oxygen. Water Research 2017; 125: 209-218.

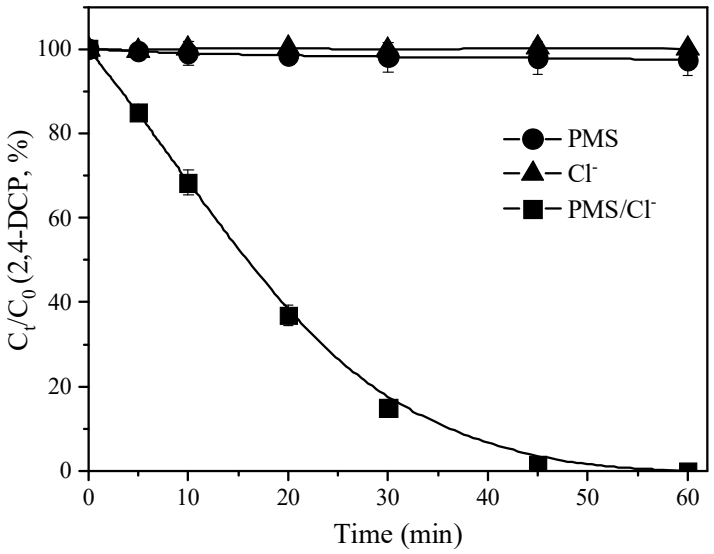

Figure 1. Degradation of 2,4-DCP in the various systems. ([2,4-DCP], 100 μM; [PMS], 2 mM; [Cl^-], 50 mM; Solution pH, 7.0; [buffer], 20 mM; stirring speed, 500 rpm)

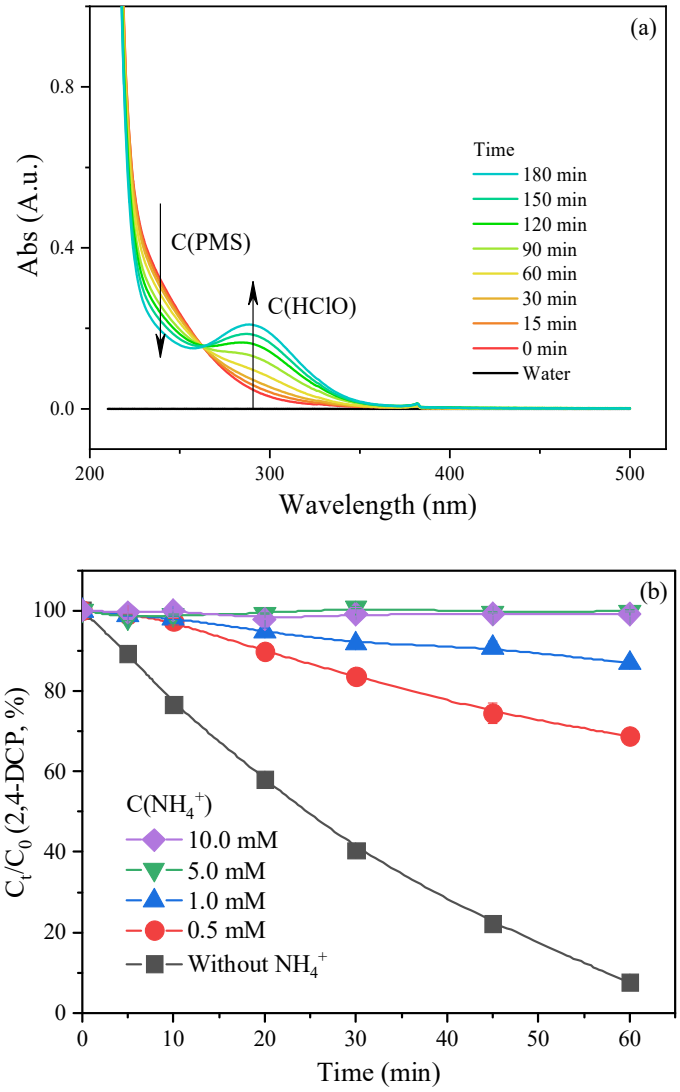

Figure 2. (a) UV-vis spectra of samples from the PMS/Cl^- process; ([PMS], 2 mM; [Cl^-], 50 mM; [buffer], 20 mM, solution pH, 7.0); (b) 2,4-DCP degradation in the presence of NH^+. ([2,4-DCP], 100 μM; solution pH 8.9)

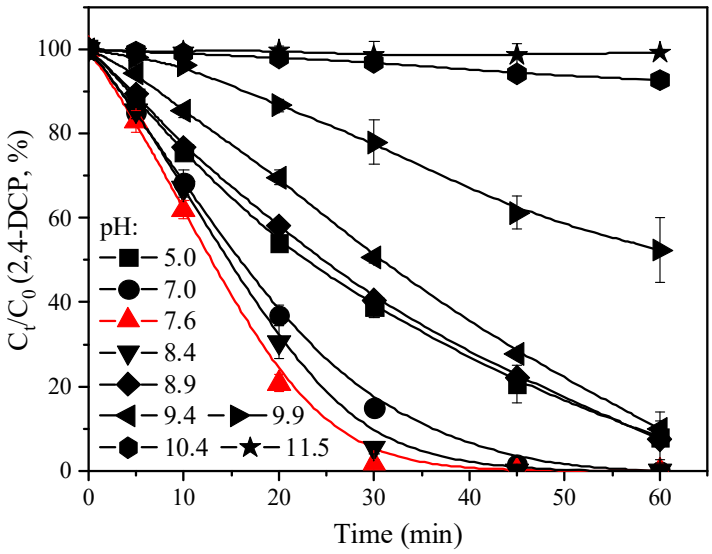

Figure 3. Effect of the solution pH on 2,4-DCP degradation in the PMS/Cl^- system. ([2,4-DCP], 100 μM; [PMS], 2 mM; [Cl^-], 50 mM; [buffer], 20 mM; stirring speed, 500 rpm)

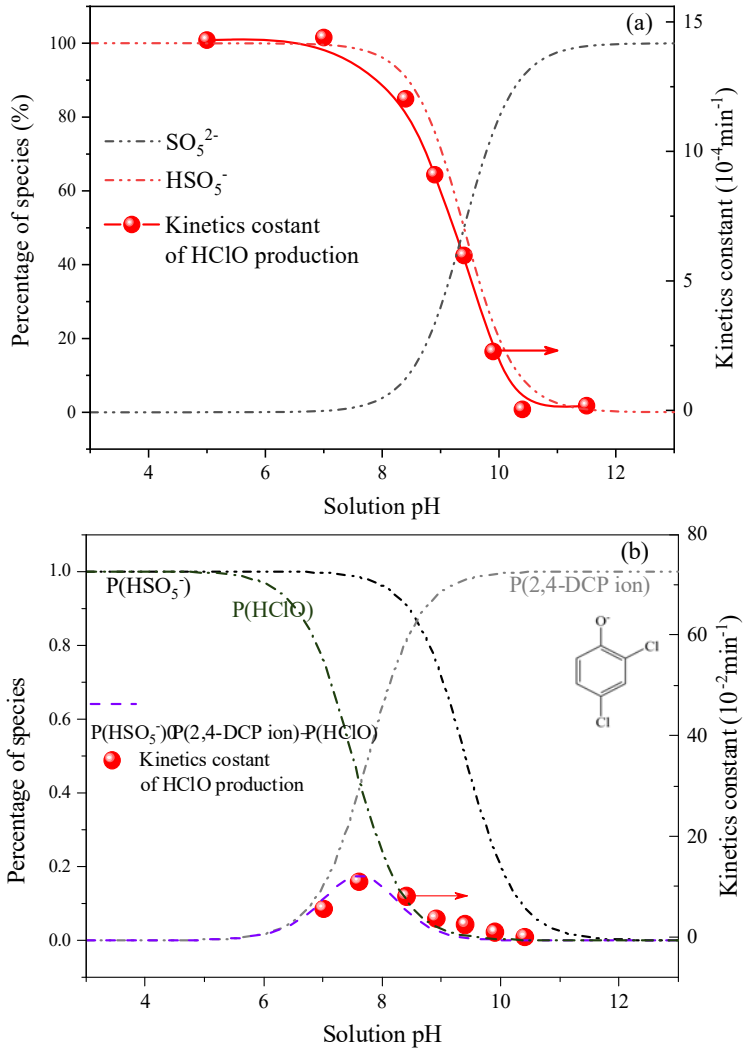

Figure 4. (a) The species distributions of PMS and the kinetics constants for HClO production in PMS/Cl^- processes. ([PMS], 2 mM; [Cl^-], 50 mM; [buffer], 20 mM; stirring speed, 500 rpm); (b) the percentage product of protonated PMS (HSO_5^-) and deprotonated 2,4-DCP (2,4-DCP ion) and the kinetics constants for 2,4-DCP degradation in PMS/Cl^- processes.

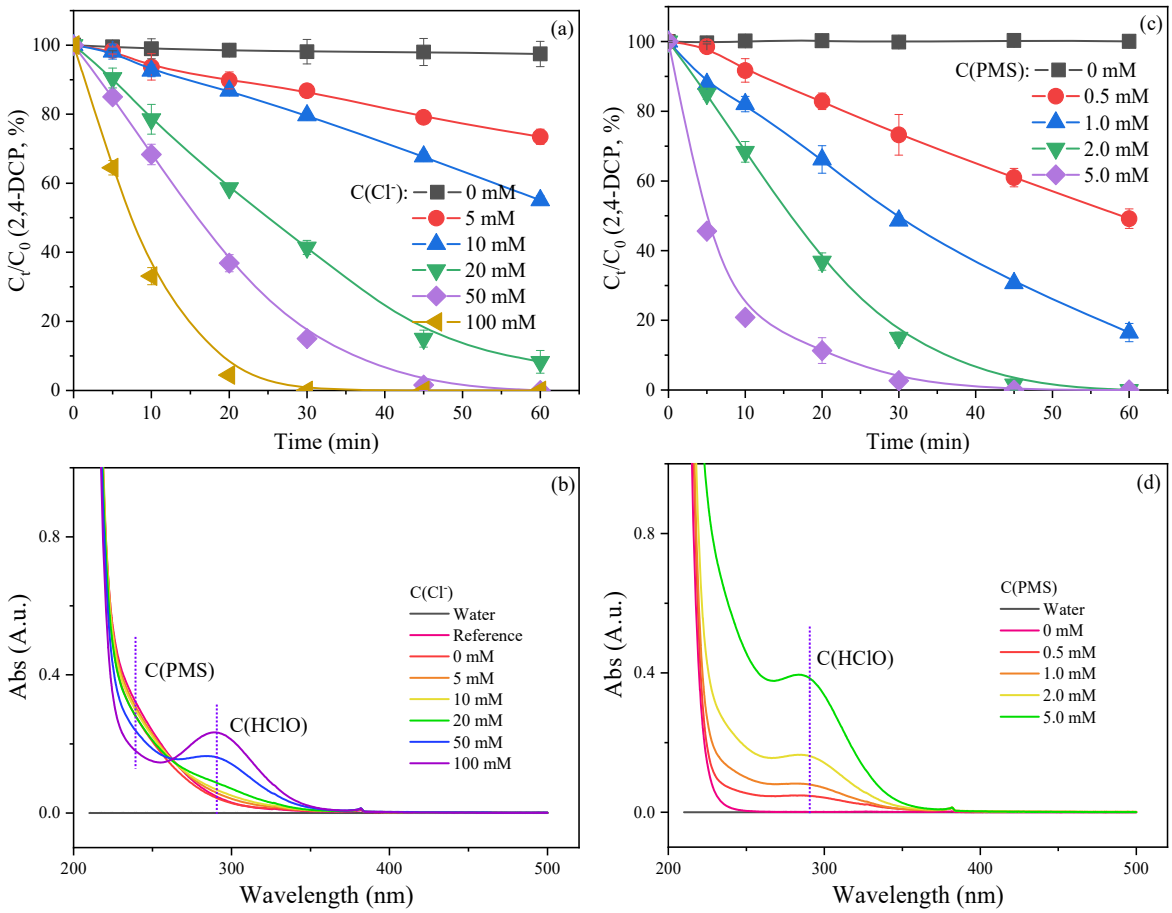

Figure 5. Effect of the Cl^- concentration on the 2,4-DCP degradation (a) and HClO production in 120 min (b); Effect of the PMS concentration on the 2,4-DCP degradation (c) and HClO production in 120 min (d); ([2,4-DCP], 100 μM (if added); [PMS], 2 mM; [Cl^-], 50 mM; [buffer], 20 mM; stirring speed, 500 rpm; solution pH, 7.0)

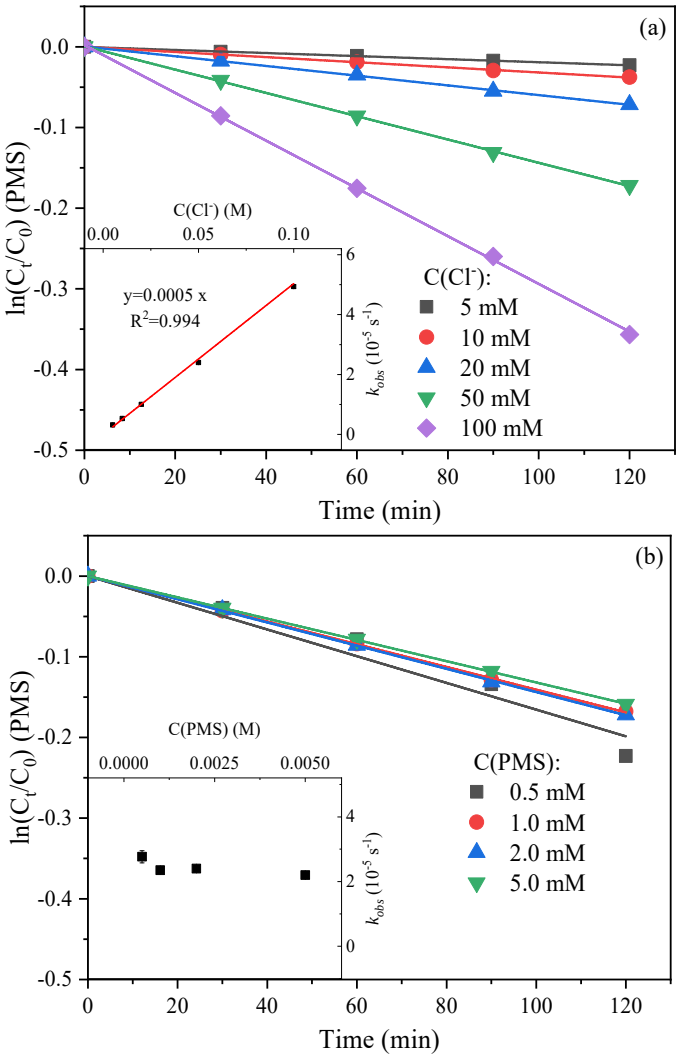

Figure 6. Effect of Cl^- (a) and PMS (b) concentrations on the PMS transformation to HClO without 2,4-DCP. ([PMS], 2 mM; [Cl^-], 50 mM; [buffer], 20 mM; solution pH, 7.0; stirring speed, 500 rpm)

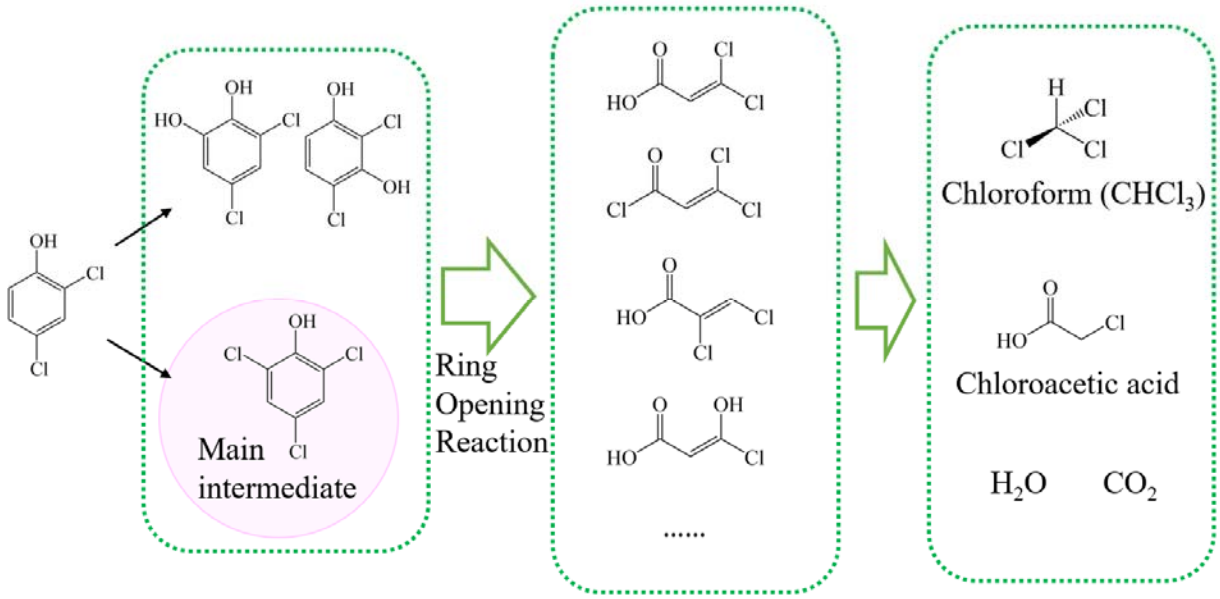

Figure. 7. Proposed degradation pathway of 2,4-DCP in the PMS/Cl^- system.